28681 DUP.

IGM88TC-205-711-G
CNRC 28681

STRUCTURE AND PROPERTIES OF A STRIP-CAST Cu-Ni-Sn AND Al-Si-Cu ALLOYS

E. Essadiqi*, J. Blain*, L. Mavropoulos** and J. Masounave*

*Industrial Materials Research Institute
75 De Mortagne
Boucherville, Quebec, Canada
J4B 6Y4

**Noranda Research Centre
240 Hymus Blvd.
Pte-Claire, Quebec, Canada
H9R 1G5

October 7th, 1988

INTRODUCTION

It is well known that casting practice has a marked influence on the properties of materials. The processes associated with high cooling rates have received enhanced interest because the latter refine the microstructure reduce microsegregation and hence improve the mechanical properties. Also these processes, such as strip casting, can eliminate a part of hot rolling, save energy and offer the possibility of new alloys as strip.

The present study uses a twin-roll caster, static mold and moving horizontal plate for strip production of C-725 copper alloy and 380 aluminum alloy. The microstructure and segregation of the thin strips of the above alloys produced under various casting conditions were characterized. The solidification time and the heat transfer between the strip and the rolls were determined.

EXPERIMENTAL PROCEDURE

The twin roll caster shown in Figure 1 was used to cast a horizontal strip. The twin rolls are made of pure copper coated with graphite with no cooling system. The radius and width of the rolls are 30 and 10 cm respectively. The chemical compositions of Cu-Ni-Sn and Al-Si-Cu alloys cast and the experimental conditions are given in Tables I and II respectively. The physical properties of the above materials are summarized in Table III. In this study the process is controlled by the speed of the rolls gradually

which is decreased from 10 RPM until the strip exists as a solid. Two systems for delivering the molten metal between the rolls were used. The Noranda system, which was used for the Cu-Ni-Sn alloy, consists of a portable induction furnace, graphite plunger and a nozzle (Figure 2). The plunger, which was always preheated to about 600°C, can be moved vertically inside the melt, thus changing its level. About 14 kg of C-725 could be delivered by this system. In the IMRI system, 150 kg of aluminum alloy was melted in an induction furnace. The melt was poured into a tundish and injected into the twin-roll caster through a refractory nozzle. The casting speed was 2 to 10 RPM depending on the material cast and on the contact angle, which was set in the range of 7 to 14 degrees. The cast strip was 1 to 2 mm in thickness and 50 to 100 mm in width.

Experiments with a static mold (Figure 3a) and a moving plate (Figure 3b) were also done with the C-725 alloy. The evolution of the specimen temperatures during solidification in the static mold was monitored by means of Chromel-Alumel thermocouples.

Evaluation

After mechanical polishing, the 380 alloy samples were etched with the following reagent [1]: $K_3Fe(CN)_6$: 5 g; $NaOH$,: 10g; H_2O: 60 ml.

The C-725 samples were etched in saturated chromic oxide solution [2]. Some samples were also examined under the JEOL scanning electron microscope.

The segregation through the thickness was investigated by microprobe analysis. Finally, the microhardness of the copper alloys was measured.

SOLIDIFICATION MODEL

Twin-roll Analysis

There is increasing interest in the mathematical simulation of a wide range of processes involving solidification, such as strip casting [3-6]. Application of the enthalpy method to the phase change phenomenon was found relatively simple and useful [7,8]. It is useful to use a one-dimensional model for the heat flow, particularly for high speed casting of thin strip [9,10], because the heat transfer in the third direction can be neglected.

Assuming steady state conditions, the general classical partial differential equation describing the heat flow within the metal is:

$$V \frac{\partial H}{\partial x} = \frac{\partial}{\partial y} \left(K \frac{\partial T}{\partial y} \right) \qquad (1)$$

where H, the enthalpy may be expressed as:

$$H \begin{cases} H_f + (T - T_l)\,\rho C_p + \rho C_p T_s & T > T_l \\ H_f \left(\frac{T - T_s}{T_l - T_s}\right) + \rho C_p T_s & T_s < T < T_l \\ \rho C_p T & T < T_s \end{cases} \qquad (2)$$

ρ is the density, c_p the specific heat, V the velocity of the strip, K the thermal conductivity and H_f the latent heat. In this model x is taken as positive in the casting direction and y as positive toward the slab centre. The melt is continuously supplied at a constant temperature To. The following simplifying assumptions were made:

- Conduction along the length of the strip and in its width direction is negligible in comparison with heat transfer in the y direction of the rolls.

- There is no slip between the strip and the rolls.

- Physical properties are temperature independent.

Using the following transformation:

$$x = V\,t \qquad (3)$$

Eq. (1) becomes:

$$\frac{\partial H}{\partial t} = \frac{\partial}{\partial y}\left(K \frac{\partial T}{\partial y}\right) \qquad (4)$$

where t is the residence time between the rolls taken for an element of volume of the strip. The above equation describes unsteady-state, one-dimensional heat conduction of the imaginary element of thin strip moving with the same velocity V. It was solved by a finite difference method using an implicit scheme.

Eq. (4) is also valid for the heat flow within the rolls, assuming the position in contact with the liquid as a plate with a given thickness.

The boundary conditions of heat transfer at the inlet, at the centre of the strip and at the roll/strip interface are given as follows:

- At the inlet the temperature of the liquid is constant and T = To.

- At the centre line of the strip, y = d/2 where d is its thickness, the heat flux is: $q = - K \frac{\partial T}{\partial y} = 0$.

- At the roll/strip interface, the heat flux is: $q = h (T - Tw)$, where h is the heat transfer coefficient between the solidified strip and roll interface, T the strip surface temperature and Tw the temperature of the roll at the interface.

Static Mold Analysis

Eq. (4) can also describe the unsteady state heat flow in a static horizontal mold assuming that the thickness of the strip is smaller than its width. In this case the boundary conditions are as follows:

- At the bottom surface of strip the heat flux is: $q = h\ (T - Tw)$.

- The heat flux at the top surface is: $q = hc\ (T - Ta) + \sigma \cdot \varepsilon \cdot (T^4 - Ta^4)$, where hc is the convection coefficient, σ the Stephan-Boltzmann constant, ε the emissivity and Ta is surrounding temperature.

RESULTS

C-725

Static Mold

1. Thermal Analysis

The variation of temperature during solidification of 4 mm thick plate of the C-725 copper alloy is given in Figure 4. It has several regions. The first shows a decrease in temperature and corresponds to undercooling. This is followed by a plateau during which solidification takes place followed by a subsequent temperature decrease [11,12]. This decrease corresponds to the

cooling of the strip by radiation and natural convection on the top surface and by heat transfer to the mold on the bottom one. The parameters defined by the thermal analysis are given in Table IV.

2. Microstructure

The microstructure of alloy C-72500, cast on a steel mold, is presented in Figure 5. In this vertical section it can be seen that the dendrite orientation and arm spacing vary as a function of distance from the bottom surface. Dendrites close to the chill surface are oriented almost vertically parallel to the heat flux to the mold for a distance of approximately 1 mm and the average secondary arm spacing is between 10 and 15 μm. Above this area, dendrites are oriented randomly with an average arm spacing between 15 and 25 μm. These differences are due to variations in the cooling rate during solidification. All samples produced statically have no particular problem with porosity and the arm spacing is finer than in the as-received material produced by continuous casting (Figure 6).

Examination of the sample shown in Figure 7 under scanning electron microscopy, revealed two new microstructural features. First, there is a considerable number of second phase particles. These precipitates (1 to 2 μm) shown in Figure 8 are much finer than those observed in the as-received material (3 to 4 μm) [13]. Chemical analysis by X-rays indicated that these precipitates consisted mainly of Cu, Ni and Sn and in some cases, they were more complex containing Cu, Ni, Sn, Zn and Fe [13].

3. Chemical Homogeneity

Two different microprobe traces for Cu, Ni and Sn were conducted for the detection of possible macro or microsegregation of the above elements. These were: i) scans across the sample thickness (Figure 9); and ii) scans across dendrite arms (Figure 10). It is evident from Figure 9 that there was no macrosegregation. Local sudden increases can be attributed mainly to the presence of second phases. However, the situation is different across the dendrite arms. As is shown in Figure 10, the Cu, Ni and Sn content changes from one dendrite arm to the next. Furthermore, when the Cu content increases, Ni decreases and Sn increases.

Dynamic Mold

1. Microstructure

The as-cast structure of 2 mm thick strip of C-725 produced with the moving mold is shown in Figure 11. It is similar in nature to the one obtained with the static mold. However, the microstructure is much more oriented parallel to the heat flow and more refined (5-13 μm). The contact between the strip and the substrate is not regular from one point to another, as can be seen in Figure 11. There is, also, a lot of porosity, particularly close to the top surface.

2. Chemical homogeneity

Microprobe scans (WDX) of C-725 across the thickness and across dendrite arms can be seen in Figures 12 and 13 and the results are similar to those reported for the static case. The only difference is that, due to the refinement in microstructure, the dendrite arm spacings and the variations in compositions are smaller.

Roll Casting

1. Microstructure and Chemical Homogeneity

A strip, 1.4 mm thick, of C-725 was produced with the twin-roll caster. The thickness uniformity of the strip is very good; however its width is not uniform. Furthermore, these samples solidified completely after they passed from the minimum roll gap and consequently, they were not deformed. The dendritic structure of the sample can be seen in Figure 14. The secondary dendrite arm spacing is between 5 and 10 μm. The structure of the sample obtained by the twin-roll process is much finer than that produced by the static and moving molds. In addition, there are second phase particles that nucleated on the dendrite arms and on grain boundaries. These precipitates are similar in nature and size to those found in the dynamic case. Through-thickness scans of the sample for Cu, Ni and Sn were conducted for the detection of possible macrosegregation. The results can be seen in Figure 15 and they are similar to what has been found already in the static and dynamic

molds.

2. Hardness

Microhardness measurements of all samples are listed in Table V. It shows the increase in hardness with the casting process from the static to the twin-roll system. This increase is the result of the structure refinement.

A380 Aluminum Alloy

The characteristic structures close to the surface and in the central zone of A380 strip are shown in Figures 16a,b respectively. When there has been good contact between the strip and the substrate, the primary dendrites of the α Al phase are parallel to the heat flow. The secondary dendrite arm spacing becomes coarser as the distance from the wheel increases. This phenomenon is related to the cooling rate as is explained later.

The microprobe profile analyses of Al, Si and Cu through the strip thickness are illustrated in Figure 17. It can be seen that the strip composition did not vary significantly from one surface to the other. However there is microsegregation with formation of a eutectic, Al-Si-Al_2Cu, which consists of Si and the intermetallic compound θ (Al_2Cu) in a matrix of aluminum solid solution [14].

DISCUSSION

C-725

All samples produced on the static mold, moving plate and twin-roll caster have the same morphology. They are dendritic in nature and they have second phase particles. However, the dendritic structure and the size of the second phase become progressively finer from the static to the dynamic to the twin-roll cast samples.

Factors affecting the dendritic structure of copper alloys include composition and cooling rate [15-17]. Increasing the solute content refines the secondary dendrite arm spacing. For a given composition, increasing the cooling rate also produces finer spacing. In the present investigation, the refinement of the dendritic structure is the result of faster cooling rates, which are related to the sample thickness and the heat transfer rates characteristic of the casting processes.

The thickness of the dynamically produced samples (≈2 mm) was almost half that of the static ones (≈4 mm). Furthermore, the average dendritic arm spacing of the dynamic sample was around 10 μm, while the average spacing for the static was 20 μm.

In the case of twin-roll cast samples, their thickness was about 1.4 mm and their average secondary arm spacing about 7 μm. The dendrite arm spacing,

as a function of the distance from the surface substrate under the three different casting processes, can be seen in Figure 18. The secondary dendrite arm spacing increases as the distance from the surface of the substrate increases, reaches a maximum and then starts decreasing again. This pattern is the result of high rate of heat extraction by the substrate which decreases as the solidification front moves away from this interface. In the case of the static and moving molds, the dendrite arm spacing decreases again at the top surface of the sample due to loss of the heat especially by radiation.

In the twin-roll process, however, the strip is solidified from both sides by the wheels. If the strip is completely solid when it leaves the rolls, this symmetry will result in a central zone corresponding to the intersection of the two solidification fronts. In the present case, this condition was not fulfilled, and at the exit, the solidified thickness was between 0.3 and 0.4 mm from both faces. Also the strip was solidifying on the surface of the lower roll after it passed from the roll gap. Therefore, the dendritic structure was not symmetrical but is rather typical of a single roll product as can be seen in Figure 18. The relationship between the secondary dendrite arm spacing (SDAS) and the distance from the roll surface can be approximately expressed as:

$$\lambda = 9 \cdot x^{0.05} \qquad (5)$$

where λ is the secondary dendrite arm spacing in μm and x is in mm.

This relation is not very accurate because of the dispersion of the SDAS with respect to distance. However, it can be used to estimate the cooling rate as will be seen later.

The horizontal moving plate can be used to study the solidification behaviour of the cast strip in the twin-roll process, particularly for a strip of 1 mm in thickness. However, Porosity due to gas entrapment in the metal during pouring of the molten metal from furnace to tundish and onto the moving mold is a problem. During such casting a thin layer of air is trapped between the mold substrate and the molten ribbon, which reduces the transfer of heat to the mold and hence reduces the cooling rate (increases the solidification time) of the strip. The improvement of microhardness due to the microstructure refinement is clear from the values given in Table V. The strip-casting process is an efficient way to improve the mechanical properties of C-725.

Microsegration

From the probe microanalysis of Cu, Ni and Sn it was found that there was no macrosegregation. However, during solidification, microsegregation appears due to partition of Ni and Sn between the solid α phase and the liquid.

The partition coefficients K_0^{Ni} and K_0^{Sn} of nickel and tin in the C-725 were estimated from the experimental results of Bastow and Kirkwood [22]. It was shown that nickel has only a small effect on K_0^{Ni} and K_0^{Sn}

whereas tin has a great influence increasing K_0^{Sn} and decreasing K_0^{Ni}. Their values in this alloy are 1.45 and 0.12 for Ni and Sn, respectively. The dendrites are rich in Ni ($K_0^{Ni} > 1$) and poor in tin ($K_0^{Sn} < 1$), which is rejected to the liquid phase. These results are shown in the microsegregation analysis.

The second phase precipitates were evident lying along dendrites and grain boundaries. Although their composition could not be accurately determined in the SEM, X-ray analysis did show that the precipitates were rich in Sn and Ni compared with the matrix.

It was assumed that these precipitates were the γ phase $(Cu_xNi_{1-x})_3$ Sn reported in other studies of Cu-Ni-Sn alloys [22].

Computer simulation

1. Static case

The variation of temperature at 0.4 mm above the surface of the substrate during solidification of 4 mm thick plate of C-725 cast on the static mold is given in Figure 4. The calculated curve from the unidimensional model is in good agreement with the experimental one. A heat tranfer coefficient varying from 2 to 1 $kW/m^2/K$ was used. These values are comparable to ones found for aluminum alloys in the range 2-1 $kW/m^2/K$ [14, 19-21]. When the plate is completely solid the heat transfer coefficient was reduced to 0.3 $kW/m^2/K$ to

fit the cooling curve. The cooling rate of the static sample varies from 17°C/s at the bottom surface to 10°C/s at the top. The rate measured from the thermal analysis was around 17°C/s.

2. Twin-roll process

Under the experimental condition described earlier, the strip was not completely solid when it left the rolls. Only 0.4 mm from each side was solid. Using the heat flow model, for residence time of 0.233 s, the value of heat transfer coefficient that fit the experimental result was found to be 6 $kW/m^2/K$. The calculated solidification time, t_f, of the strip with respect to the distance from the wheel surface is given in Figure 19. The relationship between t_f and the distance from the roll surface is given as follows:

$$t_f = 0.22\ x^{0.12} \tag{6}$$

Combining Eq. (5) and (6), a relation between the SDAS and the solidification time was expressed as:

$$\lambda = 17 \cdot t_f^{0.42} \tag{7}$$

Using the following relation:

$$t_f = \frac{T_l - T_s}{\dot{T}} \qquad (8)$$

where $\dot{T}$ is the cooling rate in °C/s and substituting this for t_f in Eq. (7), the dendrite arm spacing can be expressed with respect to the cooling rate as:

$$\lambda = 101\ \dot{T}^{-0.42} \qquad (\ )$$

The cooling rate of the strip cast C-725 was around 400°C/s.

380 Alloy

A dendritic solidification structure is characteristic of all aluminum alloy casting. The mean secondary dendrite arm spacing measurements in 380 alloy with respect to the distance from the wheel surface are illustrated in Figure 20. They are much coarser in the central zone than close to the substrate surface. The mechanical properties of cast alloys are influenced by the dendrite arm spacing [21, 23-25]. The ultimate tensile strength and elongation improve as the structure is refined. Also, an increase in the solute content up to a eutectic composition leads to a decrease in the SDAS at constant freezing rate [21, 26]. It is also well known that the SDAS decreases with decreasing solidification time (increasing cooling rate). The heat transfer coefficient that allows the strip to be completely solidified at the exit was found to be 9 $kW/m^2/K$. This value is higher than the value of

1-2 $kW/m^2/K$ in the static case. The relationship between the SDAS and the solidification time is given by [14]:

$$\lambda = 10.10\ t_f^{0.43} \tag{10}$$

where λ is in μm and t_f in seconds. Expressing t_f with respect to cooling rate T (°C/s) the above relation becomes:

$$\lambda = 38.16\ \dot{T}^{-0.43} \tag{11}$$

The cooling rates of 380 strip cast by the twin roll process vary from 400° to 100°C/s from the surface of the strip to the central zone.

CONCLUSIONS

The present investigation involved a study of the microstructure and segregation of strip cast C-725 copper alloy and 380 aluminum alloy by a vertical twin-roll caster. The following conclusions were reached:

- Macrosegregation was eliminated in Cu-Ni-Sn alloy C-725 and Al-Si-Cu 380 alloy by the twin-roll casting process, but microsegregation persisted. It is greater in the central zone, particularly for 380 alloy.

- In C-725 alloy, the secondary dendrite arm spacing depends on the cooling

rate: $\lambda = 101\ \dot{T}^{-0.42}$. For 380 alloy $\lambda = 38.16\ \dot{T}^{-0.43}$

- The cooling rates related to the strip casting process with copper rolls for C-725 and 380 alloys were found to be in the range 100-400°C/s.

- The value of the heat transfer coefficient in the casting process was found to be 9 $Kw/m^2/K$ for the 380 alloy and 6 $kW/m^2/K$ for C-725 alloy. These values are much higher than the value of 1-2 $kW/m^2/K$ in the static mold case.

- The microhardness of C-725 alloy was improved by the twin-roll process in accordance with the refinement of structure.

REFERENCES

1- R. Gruzel and W. Kurz, Metall. Trans., 18A (1987), 1137-1142.

2- Metals Handbook, "Metallography, Structures and Phase Diagrams", vol. 8, (Metals Park, OH: American Society for Metals).

3- J. Masounave, J. Blain and E. Essadiqi, "Séminaire sur les nouvelles applications de l'acier face à concurrence des matériaux de substitution" (Paper presented at the Commission Économique pour l'Europe, Luxembourg, May 2 to 6, 1988).

4- M.J. Bagshaw, J.D. Hunt and R.M. Jordan, Modelling and Control of Casting and Welding Processes", TMS/AIME, Warrendale, Pa., (1988), 135-147.

5- R.J. O'Malley and M.E. Karabin, "Modeling and Control of Casting and Welding Processes", TMS/AIME, Warrendale, Pa., (1986), 149-168.

6- Y.G. Kim, B. Farouk and J. Keverian, "Manufacturing Simulation and Processes, ASME, 20, (1986), 256-259.

7- V. Voller and M. Cross, "Int. J. Heat Mass Transfer", 24 (1981), 545-556.

8- E.M. Gutierrez and J. Szekely, Metall. Trans., 17B (1986), 695-703.

9- I. Jin and J.G. Sutherland, "Solidification and Casting of Metals, Metal Society, London, (1979), 256-259.

10- T.W. Clyne, Metall. Trans., 15B (1984), 369-381.

11- Kjell-Olof Jonsson, Jern. Kont. Ann., 153 (1969), 193-199.

12- L.M.D. Schetky, L. Backerud, L.M. Liljenvalla and H. Steen, AFS Transactions, 91 (1983), 137-144.

13- L.T. Mavropoulos and G. Deep, Noranda Report, Noranda Research Centre, Montreal, Quebec (1988).

14- E. Essadiqi, J. Blain and J. Masounave, "Solidification Structure of a Strip Cast Al-Si-Cu Alloys", in proceedings "Reduction and Casting of Aluminium, C. Bickert, ed., CIMM, vol. 8 (1988), 131-146.

15- L. Backerud and L.M. Liljeuvaill, "Copper and its Alloys", Institute of Metals, London, Monograph and Report Series No. 34, (1970), 65.

16- L. Backerud and L.M. Liljeuvaill, "The Solidification Characteristics of 7 Constitutionally Different Types of Binary Copper Alloys", INCRA - project 165, Swedish Institute for Metal Research, Stockholm, 1971.

17- T.F. Bower and M.R. Randlett, "Solidification Structures of Copper Alloy Ingots", Metals Handbook, vol.9 (Metals Park, OH: American Society for Metals, 1985), 637-645.

18- H.H. Liebermann, "Gas Boundary Layer Effect in Processing Glassy Alloy Ribbons", Rapidly Quenched Metals III, vol. 1, B. ed., B. Cautor (London, England, The Metals Society, 1978), (1978), 34-40.

19- L.J.D. Sully, Trans AFS, 84 (1976), 735-744.

20- K. Ho and R.K. Pehlke, Metall. Trans., 16B, (1985), 585-594.

21- M. Bamberger, B.Z. Weiss and M.M. Stuper, Met. Sci. and Tech., 3 (1987), 49-56.

22- B. Bastow and D. Kirkwood, J. Int. Metals, 99 (1971), 277-283.

23- R. Elliot, "Eutectic Solidification Processing", Butterworths, ed., (1983), 182-188.

24- G.R. Armstrong and H. Jones, "Solidification and Casting of Metals", Metal Society, London, (1979), 454-458.

25- K.J. Oswald and M.S. Misra, AFS International, Cast-Metal J., 6 (1981), 23.

26- S.F. Frederick and W.A. Baily, Trans. Metall. Soc., AIME, 242 (1968), 2063.

27- K.P. Young and D.H. Kirkwood, Metall. Trans., 6A (1975), 197-205.

28- Metals Handbook, "Properties and Selection - Non Ferrous Alloys and Pure Metals", vol. 9 (Metals Park, OH: American Society for Metals), 170, 378.

Table I. Chemical Composition (%wt) of Cu-Ni-Sn (C-725 Alloy) and Al-Si-Cu (380 Alloy)

C-725	Cu	Ni	Sn	Fe	Zn	Mn	Pb
	Rem.	8.5-10.5	1.8-2.8	0.6	0.5	0.2	0.05
380	Al	Si	Cu	Zn	Fe	Mg	
	Rem.	9.16	3.25	2.41	0.84	0.05	

Table II. Experimental Conditions of C-725 and 380 Alloys

Alloy	Casting Process	T_0, °C	Speed	Contact Angle Degree	Thickness (mm)
C-725	Static mold	1180	--	--	4
	Moving mold	1140	40 cm/s	--	2
	Twin roll	1170	5 (RPM)	7	1.4
380	Twin roll		5 (RPM)	7	2

Table III. Physical Properties of C-725 and 380 Alloys [28]

Materials	C-725	380
Density (kg/m^3)	8890	2740
Liquidus T_l (°C)	1130	572[a]
Solidus T_s (°C)	1060	550[a]
Latent heat (Kj/kg)	210[b]	389
Specific heat (J/kg·K)	541	963
Thermal conductivity (W/m·K)	55	96.2

(a): these values have been determined experimentally
(b): the heat of fusion of C-725 was estimated from the weighted averages of the pur elements of the alloy

Table IV. Thermal Analysis of the C-725 Strip Cast in Static Case

Undercooling	:	60°C
Solidification temperature	:	1072
Solidification time	:	4 s

Table V. Microhardness of C-72500 As-Cast in Static, Dynamic and Twin-Roll Processes

Casting Process	Vickers Hardness (HV)
Static	79
Dynamic	94
Twin-roll	108

LIST OF FIGURES

Figure 1 - Twin-roll strip caster (schematic).

Figure 2 - Metal delivery system for the twin-roll experiments with alloy C-725.

Figure 3 - a) Static steel mold and. b) Moving plate caster section.

Figure 4 - Cooling curve of C-725 copper alloy, 4 mm in thickness, cast on static mold.

Figure 5 - As-cast structure of C-725 across the thickness showing columnar and equiaxed dendrites, static case.

Figure 6 - Structure of the as-received C-725 alloy.

Figure 7 - Microstructure of C-725 copper alloy cast on static mold, observed under scanning electron microscope.

Figure 8 - SEM micrograph of C-725 alloy showing precipitates rich in Ni and Sn.

Figure 9 - The distribution of Cu, Ni and Sn across the thickness of the as-cast C-725 cast under static conditions.

Figure 10 - The distribution of Cu, Ni and Sn across the dendrite arms indicated in the SEM micrograph of C-725 cast on static steel mold.

Figure 11 - As-cast structure through a thickness of C-725 copper alloy cast on the horizontal moving plate.

Figure 12 - The distribution of Cu, Ni and Sn through the thickness of C-725 alloy cast on the moving plate.

Figure 13 - The distribution of Cu, Ni and Sn across the dendrite arms shown in SEM micrograph of C-725 cast on the moving plate.

Figure 14 - As-cast structure of C-725 copper alloy across the thickness, cast by the twin-roll process.

Figure 15 - The distribution of Cu, Ni and Sn across the thickness of a strip cast C-725 alloy.

Figure 16 - a) As-cast structure of 380 aluminum alloy close to the wheel surface. b) As-cast structure of 380 aluminum alloy at the centre of the strip.

Figure 17 - The distribution of Al, Si and Cu across the thickness of the as-cast 380 aluminum alloy.

Figure 18 - The dendrite arm spacing vs. distance from the mold for C-725 copper alloy cast in different molds.

Figure 19 - Solidification time, t_f, with respect to the distance from one wheel surface to 0.4 mm thickness of the strip C-725 alloy.

Figure 20 - The average dendrite arm spacing vs. distance from one wheel surface for 380 aluminum alloy.

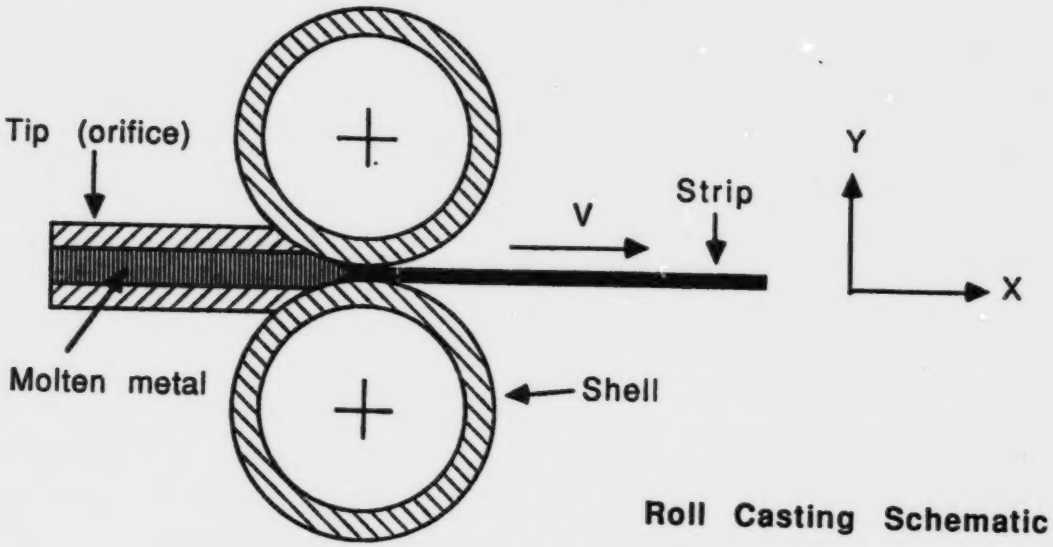

TWIN-ROLL STRIP CASTER (SCHEMATIC)

Fig-1

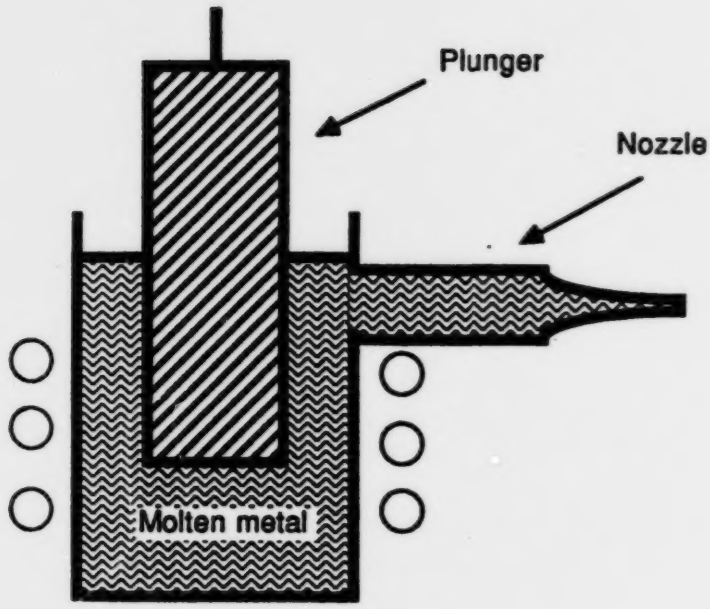

IETAL DELIVERY SYSTEM FOR THE TWIN-ROLL EXPERIMENT WITH ALLOY C-725

Fig 2

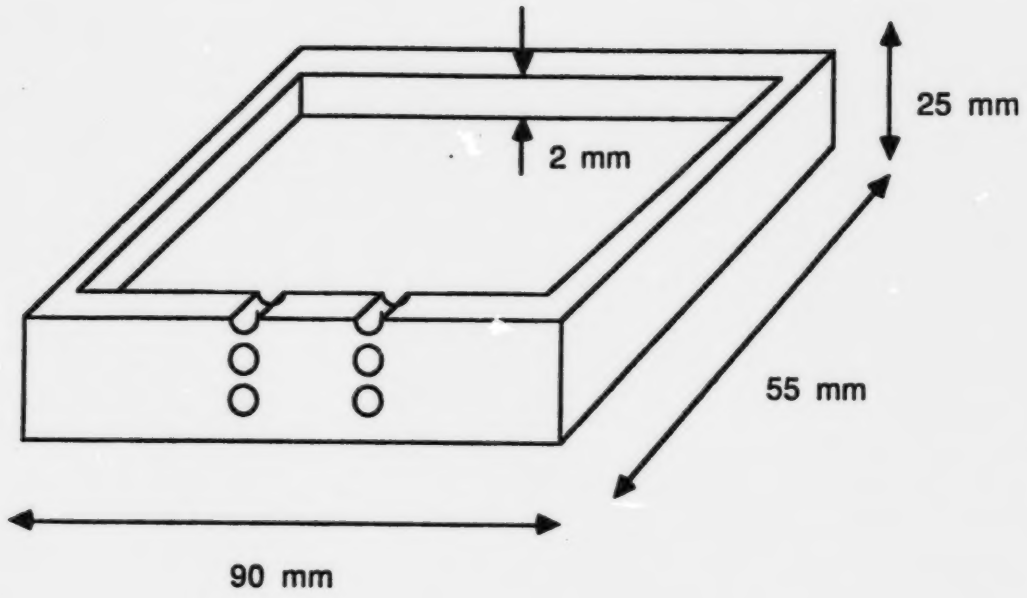

STATIC STEEL MOLD

Fig 3 a

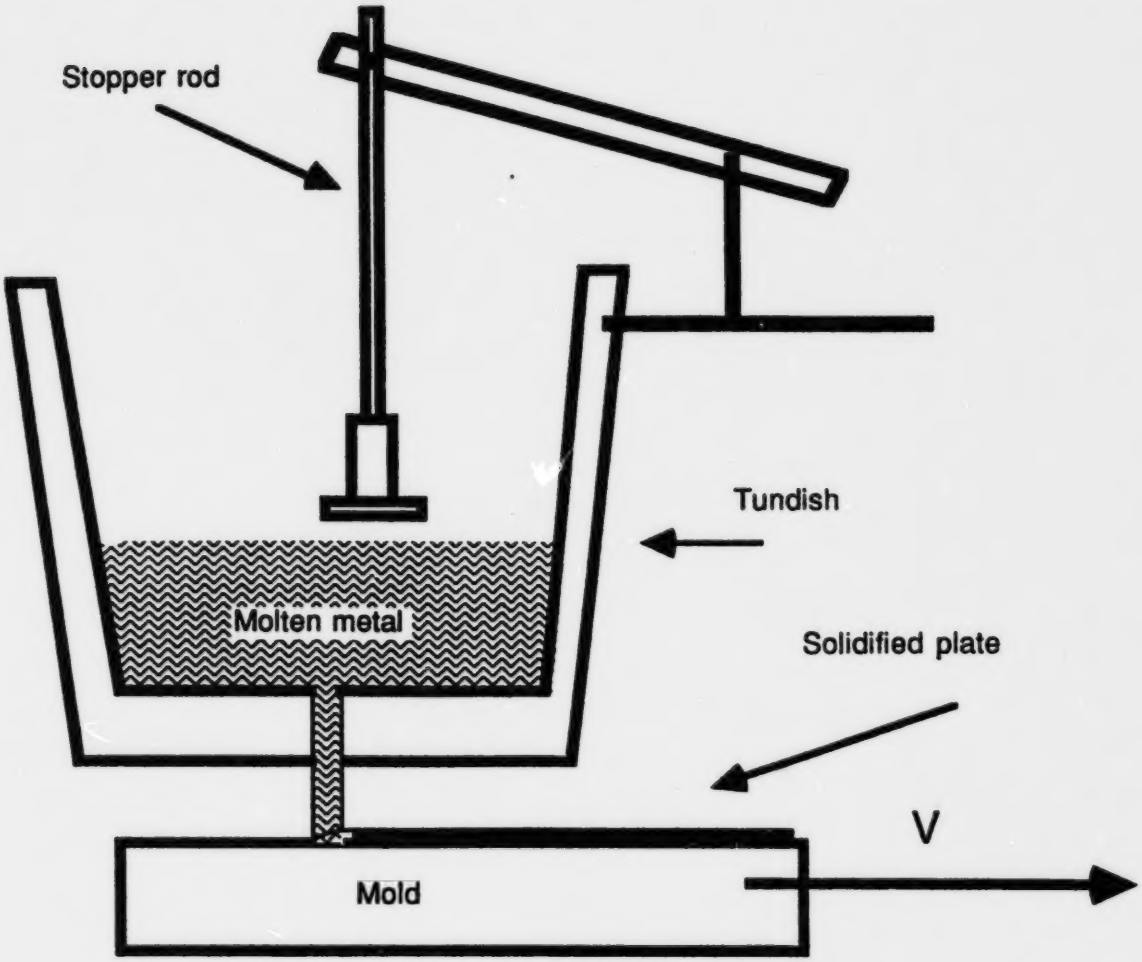

MOVING PLATE CASTER SECTION

Fig 3b

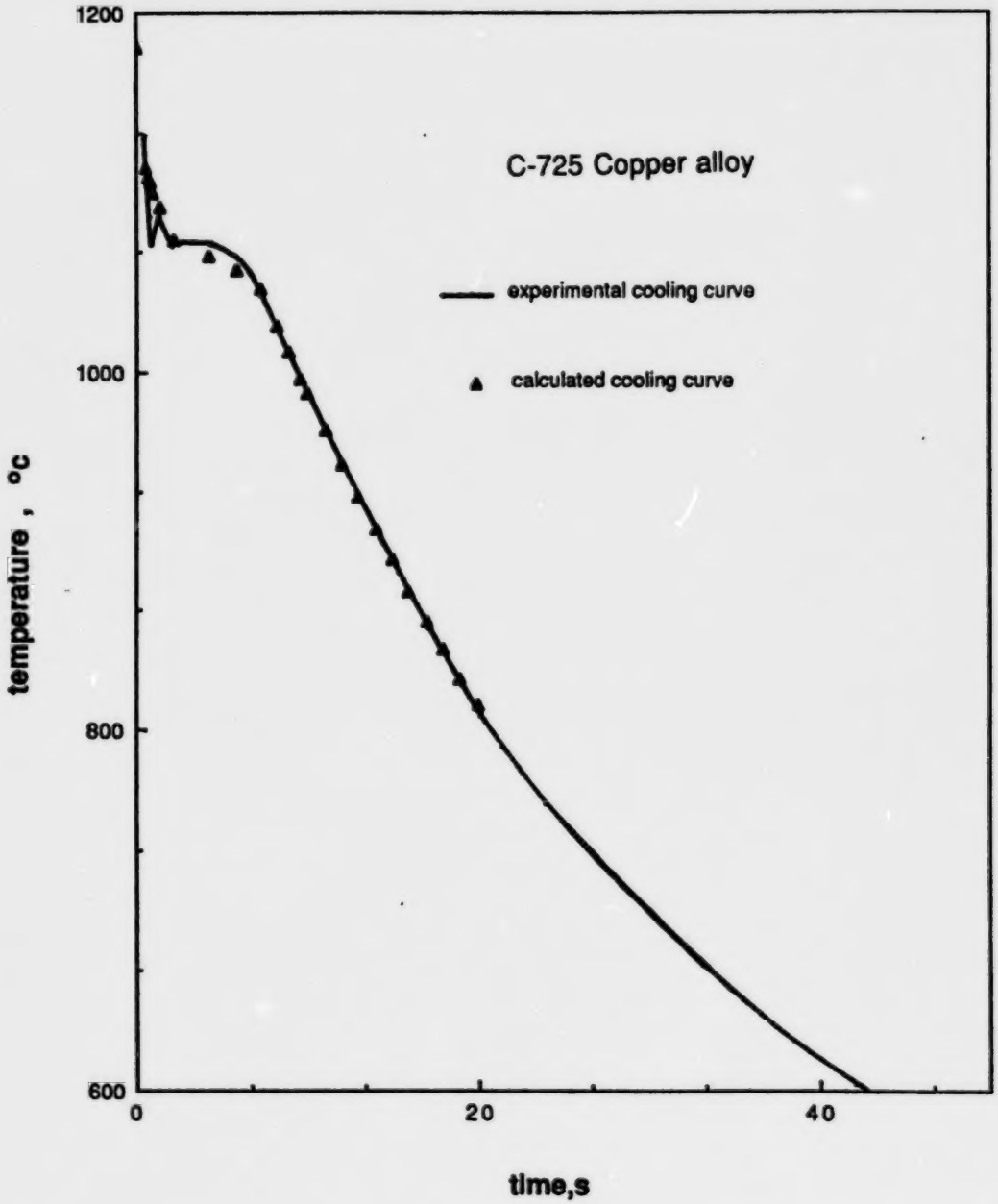

COOLING CURVE OF C-725 COPPER ALLOY,
4 mm IN THICKNESS, CAST ON STATIC MOLD

Fig 4

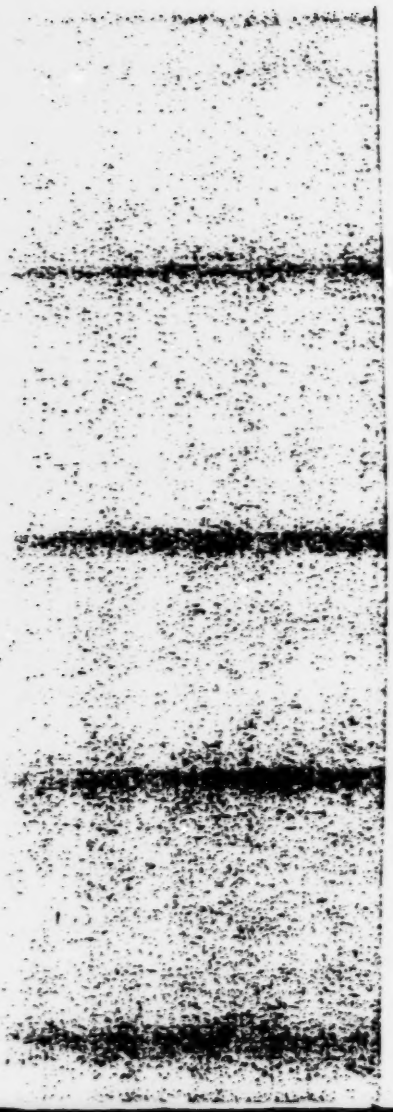

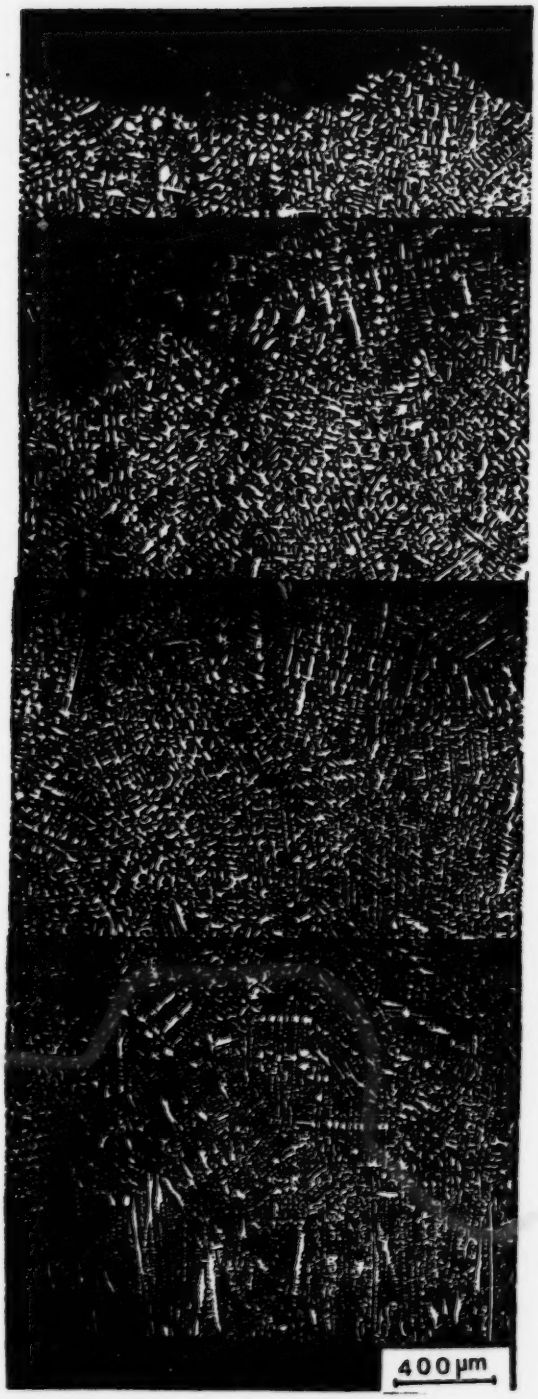

AS-CAST STRUCTURE OF C-725 ALLOY ACROSS THE THICKNESS, SHOWING COLUMNAR AND EQUIAXED DENDRITES, STATIC CASE

Fig 5

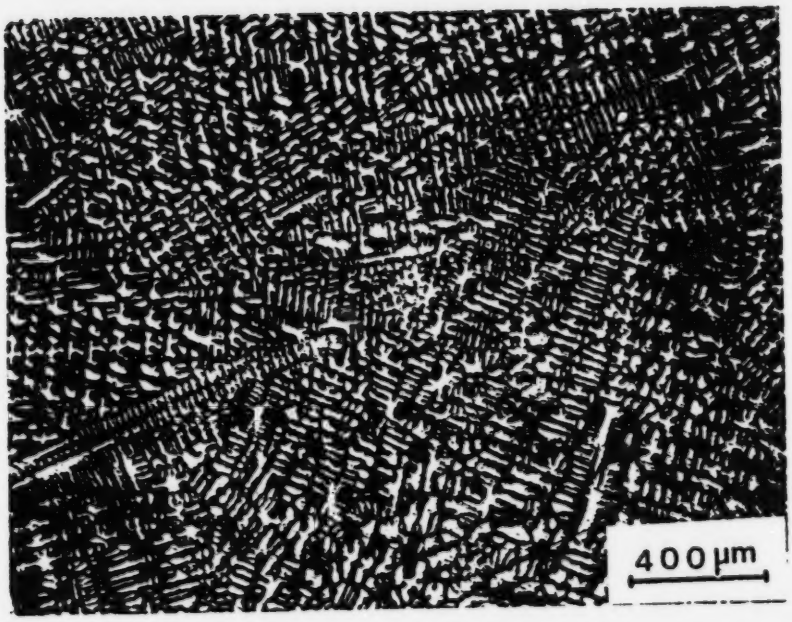

STRUCTURE OF THE AS-RECEIVED C-725 ALLOY

Fig - 6

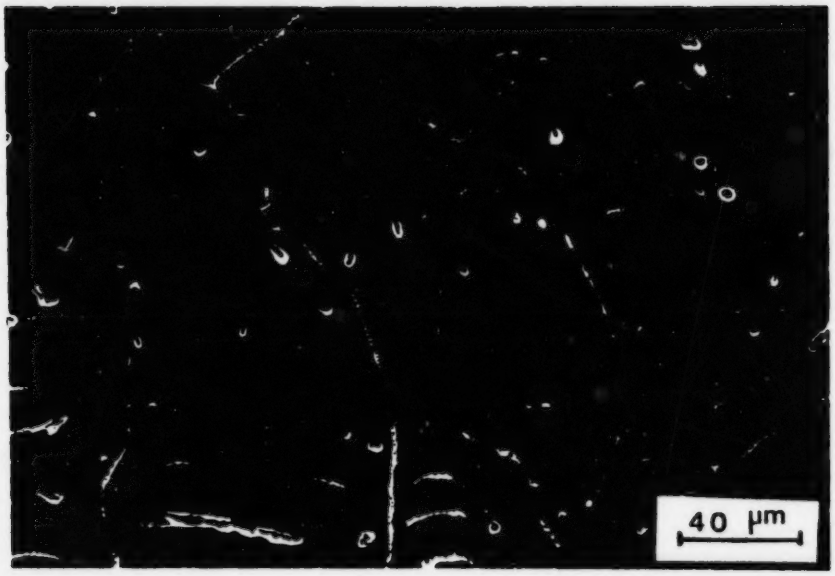

MICROSTRUCTURE OF C-725 ALLOY CAST ON STATIC MOLD,
OBSERVED ON SCANNING ELECTRON MICROSCOPE

Fig 7

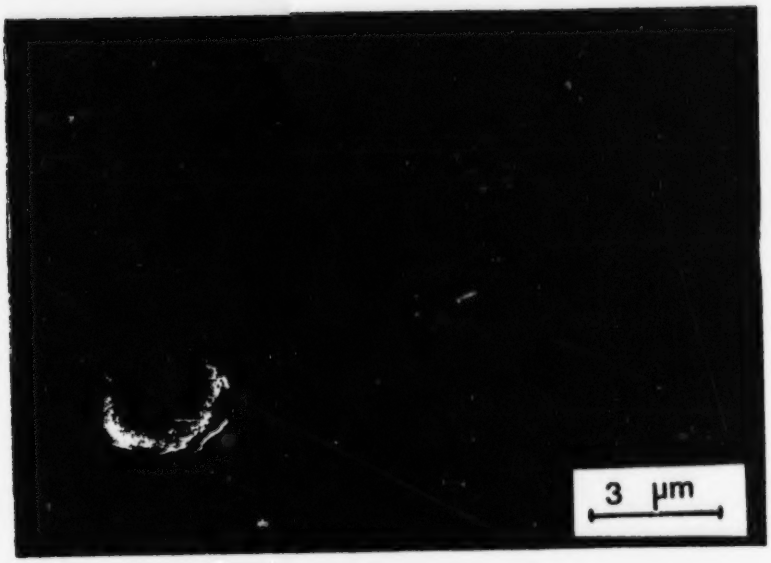

SEM MICROGRAPH OF C-725 ALLOY
SHOWING PRECIPITATES RICH IN Ni AND Sn

Fig 8

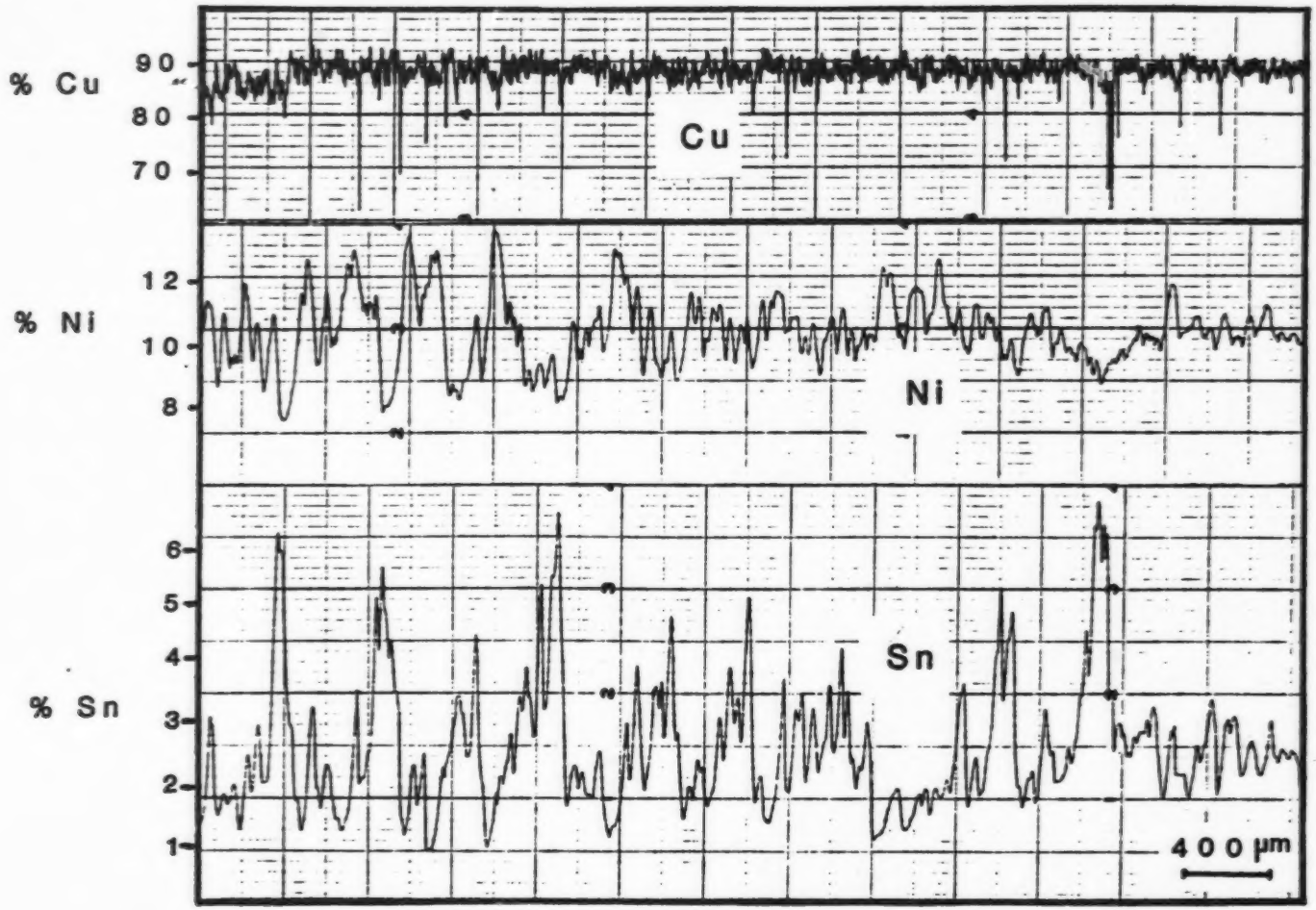

THE DISTRIBUTION OF Cu Ni AND Sn ACROSS

THE THICKNESS OF THE COPPER ALLOY C-725

STATIC CASE

Fig-9

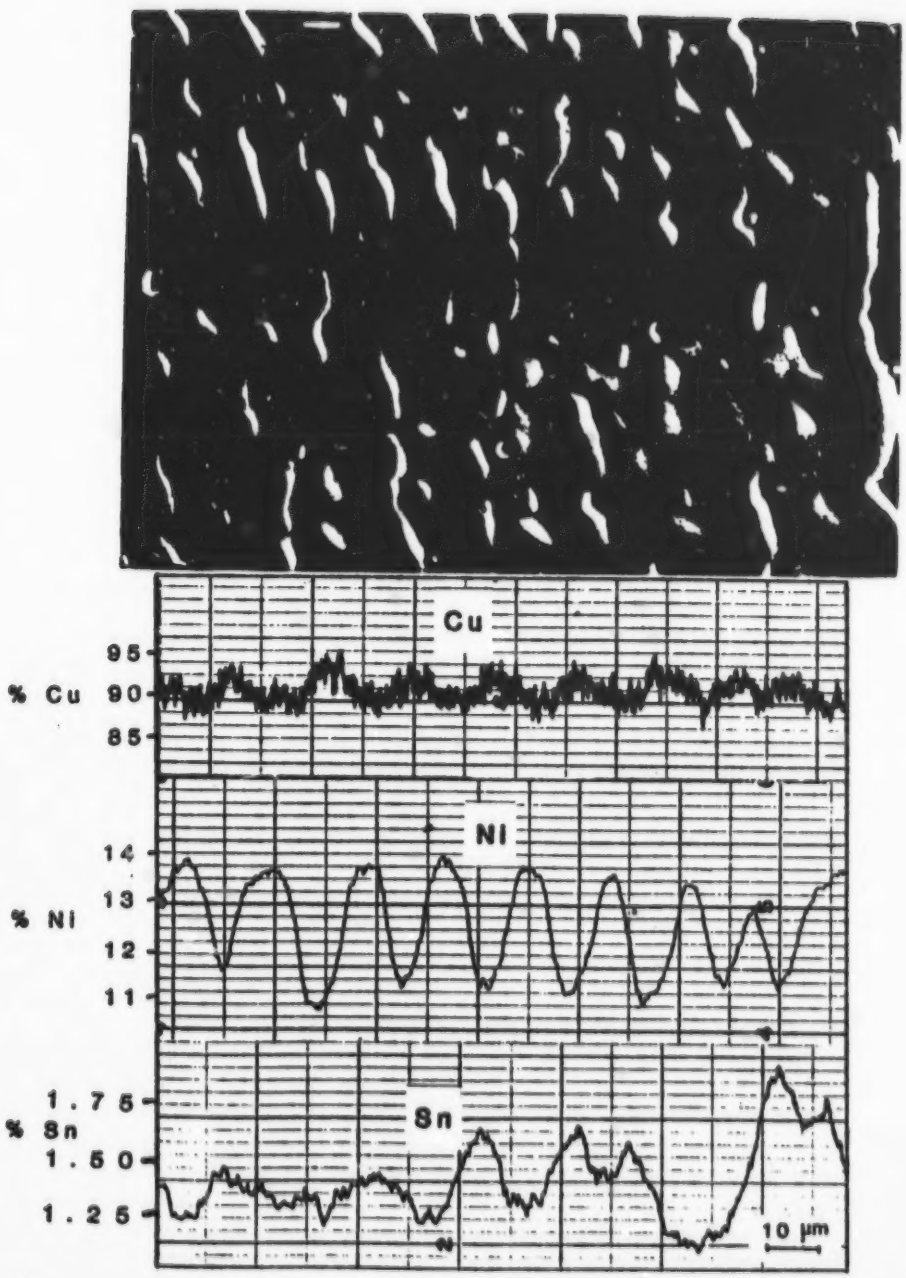

Fig - 10

DISTRIBUTION OF Cu, Ni AND Sn ACROSS THE DENDRITE ARMS AS INDICATED IN THE SEM MICROGRAPH OF C-725 CAST ON STATIC STEELMOLD

AS-CAST STRUCTURE THROUGH THE THICKNESS OF C-725 ALLOY CAST ON THE HORIZONTAL MOVING PLATE

Fig - 11

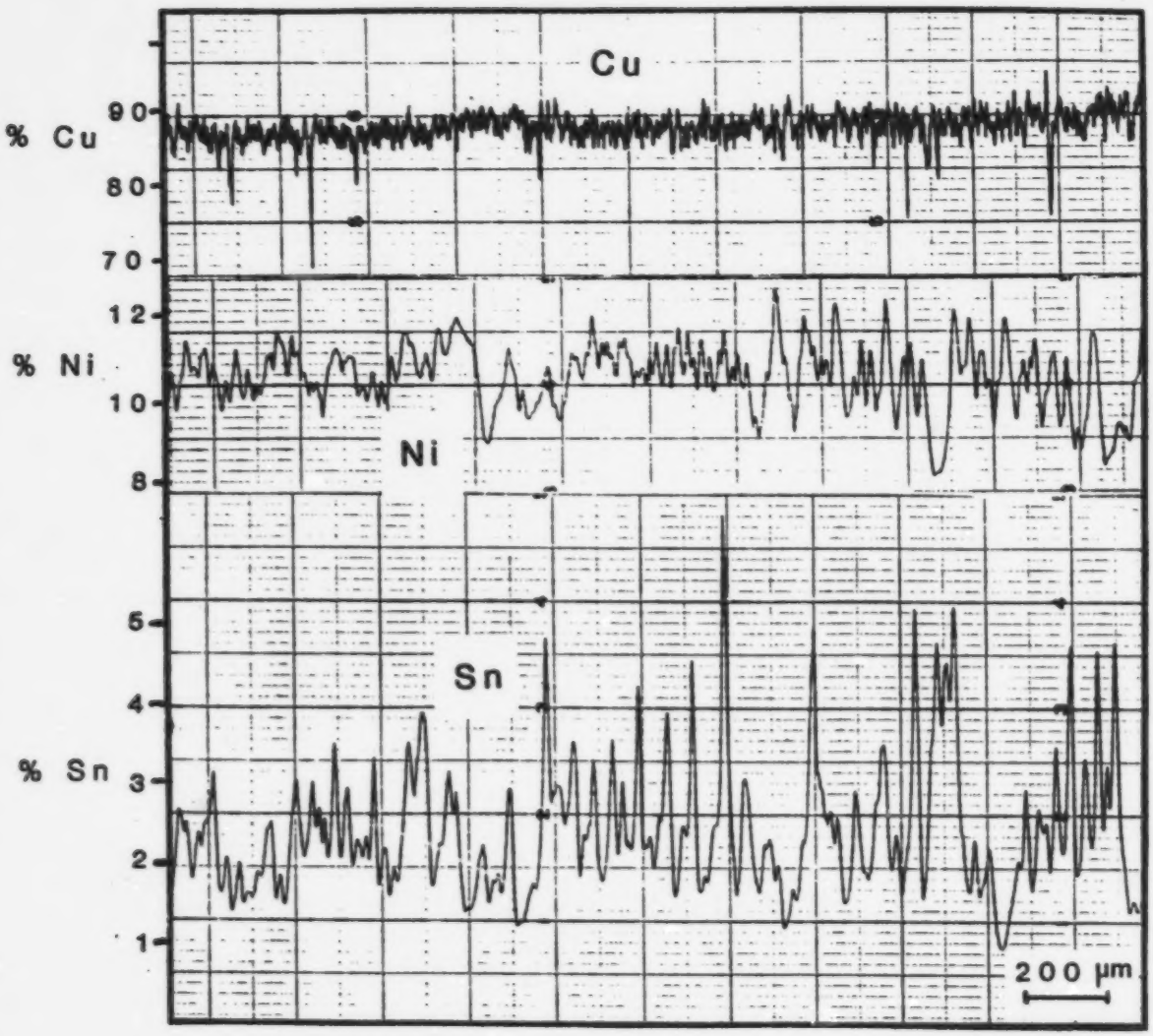

THE DISTRIBUTION OF Cu Ni AND Sn ACROSS THE THICKNESS OF THE COPPER ALLOY C-725 DYNAMIC CASE

Fig - 12

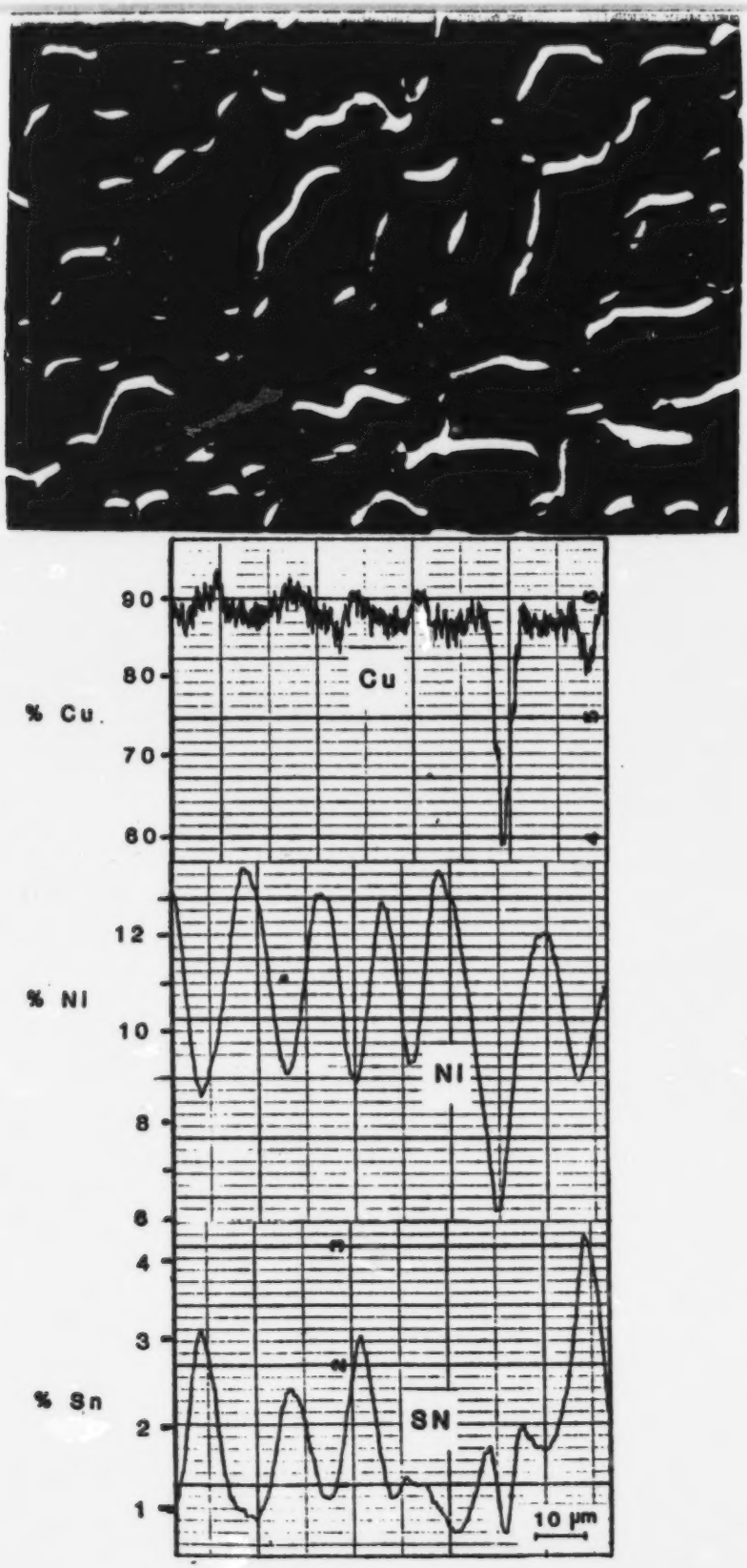

Fig-13

DISTRIBUTION OF Cu, Ni AND Sn ACROSS THE DENDRITE ARMS SHOWN IN THE SEM MICROGRAPH OF C-725 ALLOY CAST ON THE HORIZONTAL MOVING PLATE

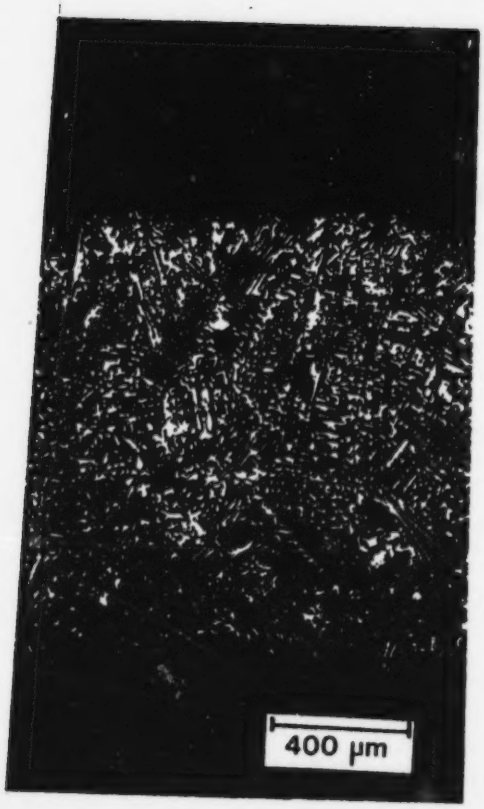

AS-CAST STRUCTURE OF C-725 ALLOY ACROSS THE THICKNESS,
CAST BY THE TWIN-ROLL PROCESS

Fig -14

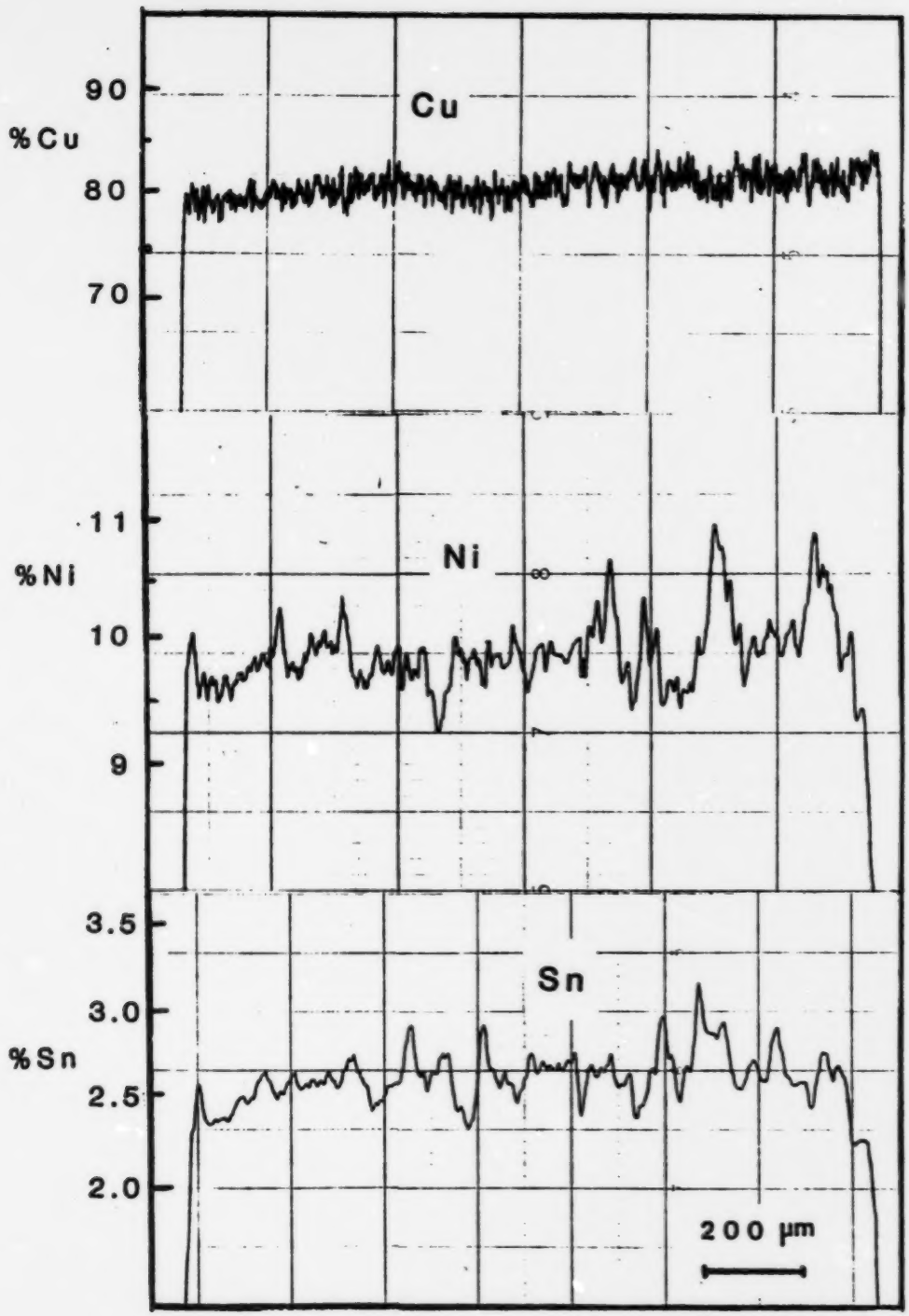

DISTRIBUTION OF Cu, Ni AND Sn ACROSS THE THICKNESS OF A STRIP CAST C-725 ALLOY

Fig-15

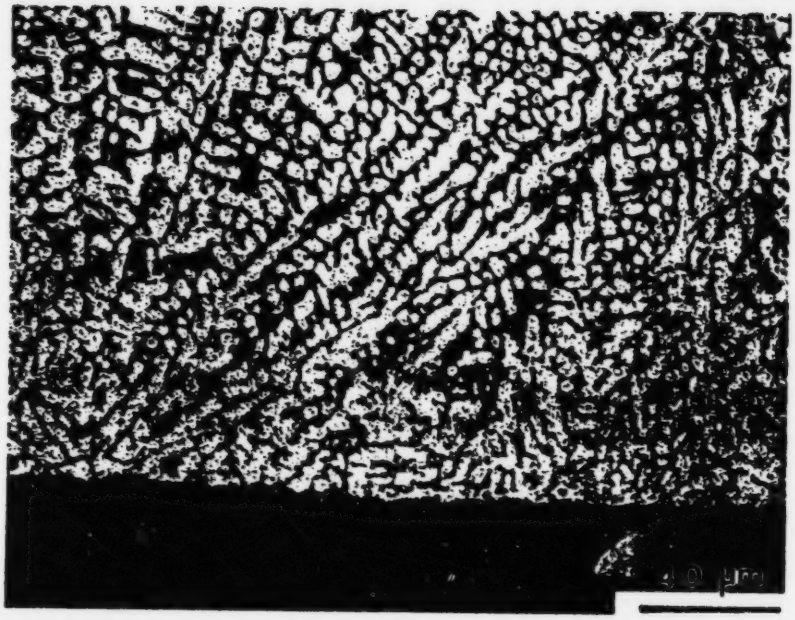

a) AS-CAST STRUCTURE OF 380 ALUMINUM ALLOY CLOSE TO THE WHEEL SURFACE

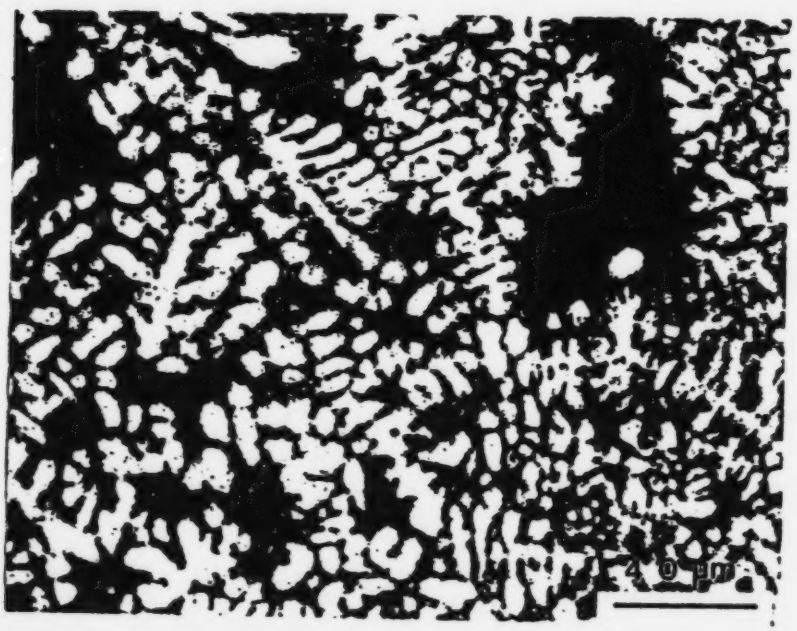

b) AS-CAST STRUCTURE OF 380 ALUMINUM ALLOY AT THE CENTER OF THE STRIP

Fig - 16a, b

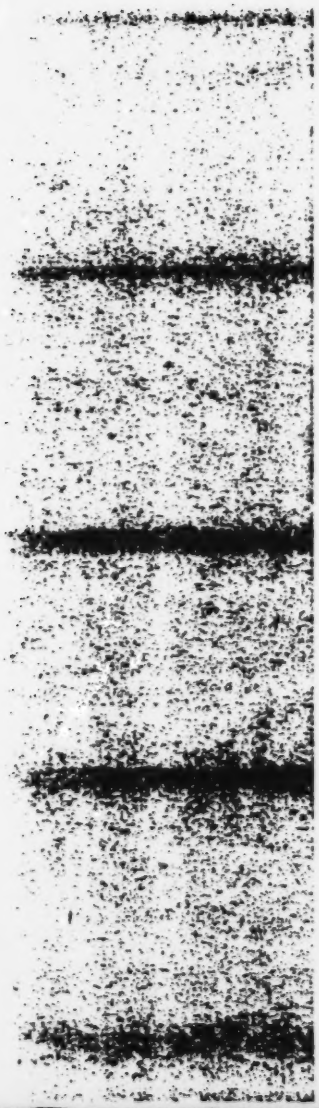

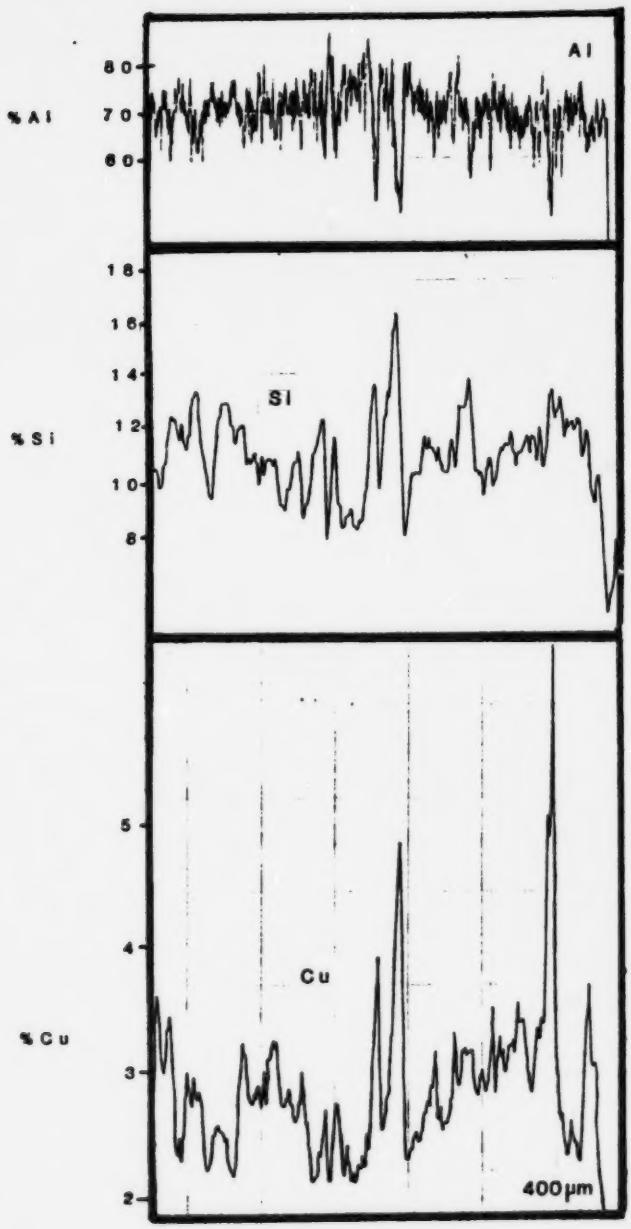

THE DISTRIBUTION OF Al, Cu AND Si ACROSS THE THICKNESS OF THE AS-CAST ALUMINUM ALLOY

Fig-17

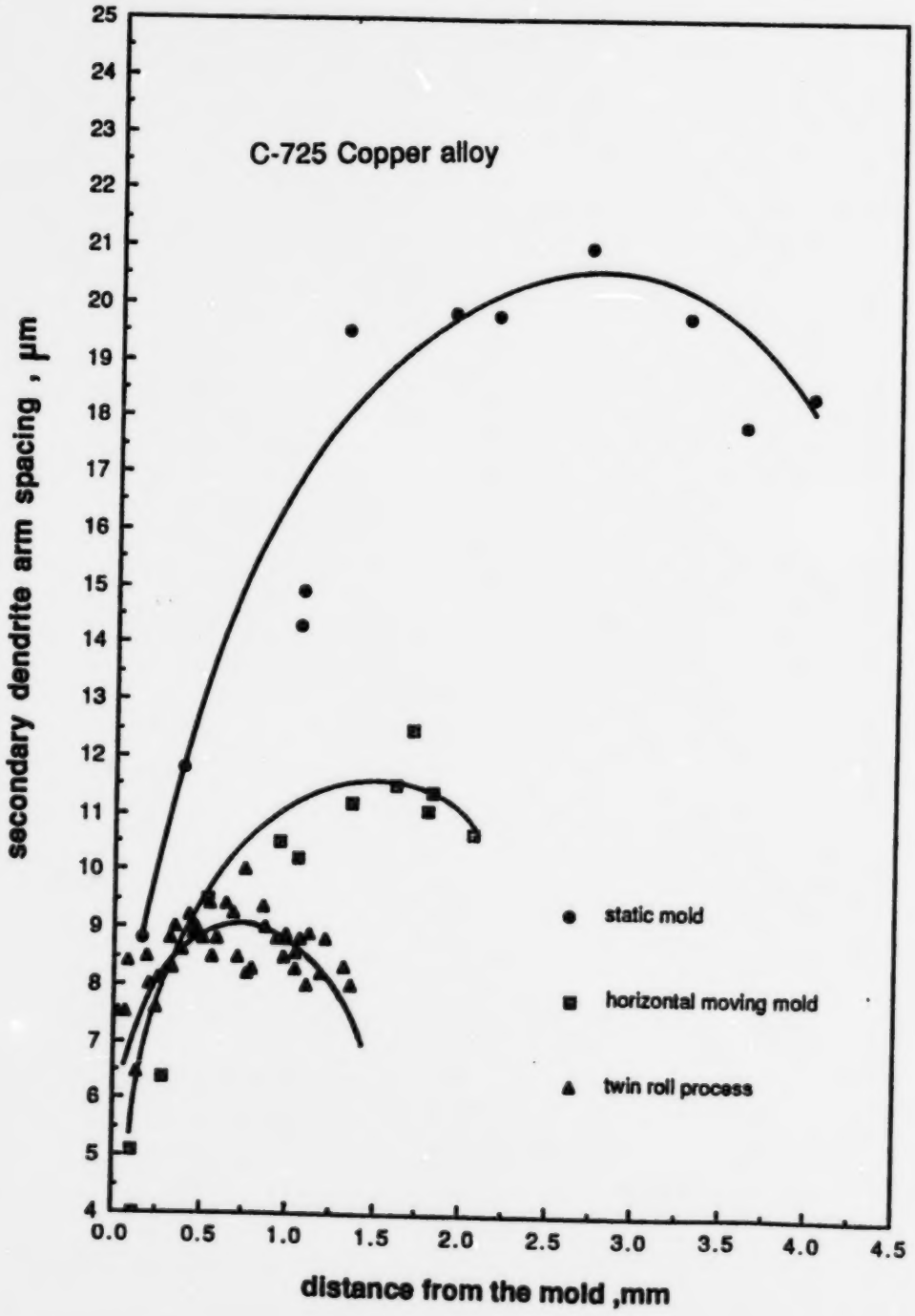

THE DENDRITE ARM SPACING vs THE DISTANCE FROM THE MOLD FOR C-725 COPPER ALLOY CAST IN DIFFERENT MOLDS

Fig - 18

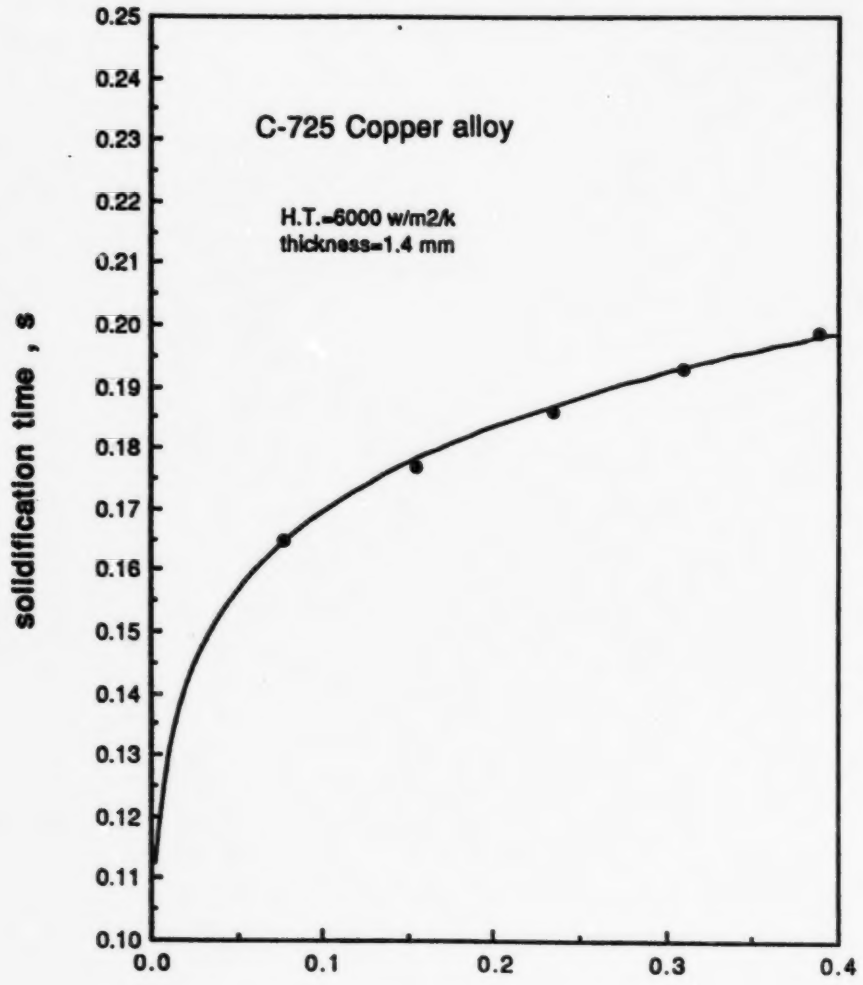

SOLIDIFICATION TIME, t_f, WITH RESPECT TO THE DISTANCE FROM ONE WHEEL SURFACE TO 0.4 mm THICKNESS OF THE STRIP C-725 COPPER ALLOY

Fig - 19

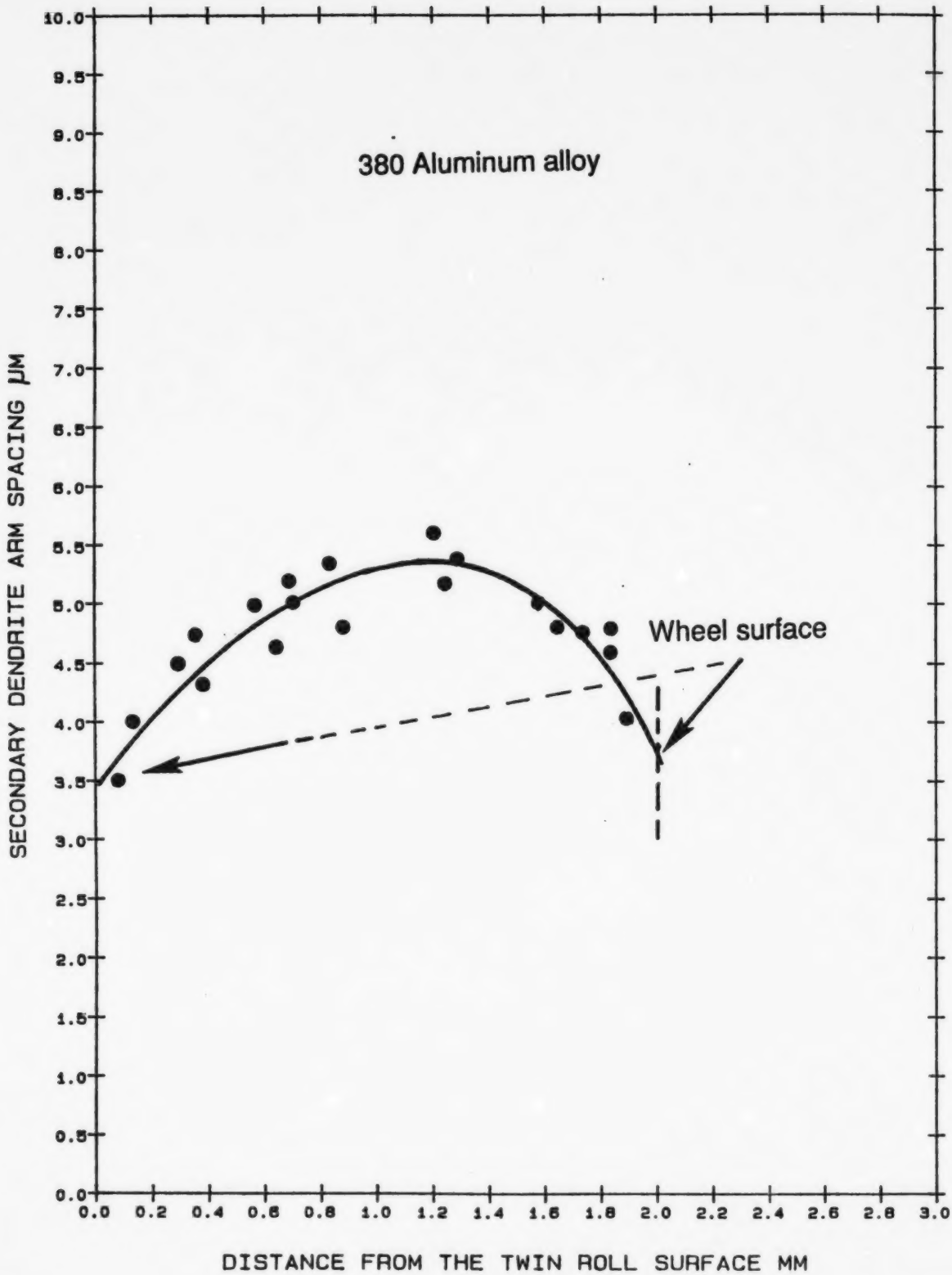

DENDRITE ARM SPACING VERSUS DISTANCE FROM ONE WHEEL SURFACE FOR THE AS-CAST 380 ALLOY

Fig-20